**Atmospheric
Chemistry
and Physics
Discussions**

Large scale changes in 20th century black carbon deposition to Antarctica

M. M. Bisiaux[1], R. Edwards[1,2], J. R. McConnell[1], M. A. J. Curran[3,4], T. D. Van Ommen[3,4], A. M. Smith[5], T. A. Neumann[6], D. R. Pasteris[1], J. E. Penner[7], and K. Taylor[1]

[1]Desert Research Institute, Reno, NV, USA
[2]Curtin University, Perth, WA, Australia
[3]Australian Antarctic Division, Kingston, TAS, Australia
[4]Antarctic Climate and Environment CRC, University of Tasmania, Hobart, TAS, Australia
[5]Australian Nuclear Science and Technology Organisation, Lucas Heights, NSW, Australia
[6]Goddard Space Flight Center, NASA, Greenbelt, MD, USA
[7]University Michigan, Ann Arbor, MI, USA

Correspondence to: M. M. Bisiaux (marion.bisiaux@dri.edu)

Large scale changes in 20th century black carbon deposition to Antarctica

M. M. Bisiaux et al.

Title Page

Abstract	Introduction
Conclusions	References
Tables	Figures

|◄ | ►|
◄ | ►

Back | Close

Full Screen / Esc

Printer-friendly Version

Interactive Discussion

Abstract

Refractory black carbon aerosols (rBC) emitted by biomass burning (fires) and fossil fuel combustion, affect global climate and atmospheric chemistry. In the Southern Hemisphere (SH), rBC is transported in the atmosphere from low latitudes to Antarctica and deposited to the polar ice sheet preserving a history of emissions and atmospheric transport. Here, we present two high-resolution Antarctic rBC ice core records drilled from the West Antarctic Ice Sheet divide and Law Dome on the periphery of the East Antarctic ice sheet. Separated by ∼3500 km, the records span calendar years 1850–2001 and reflect the rBC distribution over the Indian and Pacific ocean sectors of the Southern Ocean. Highly correlated over the past 60 yr, the records show that coherent large-scale changes in SH rBC occurred at decadal to inter-annual time scales, notably in ENSO-like periodicities. Decadal trends in the records are similar to inventories of SH rBC emissions from grass fires and biofuels. The combined records suggest a large-scale reduction in rBC from 1950 to 1990 over the remote Southern Hemisphere.

1 Introduction

Refractory black carbon (rBC, soot) aerosols are present in the Antarctic atmosphere, snow and ice (Chýlek et al., 1987; Warren and Clarke, 1990; Chýlek et al., 1992; Grenfell et al., 1994). These aerosols are the result of long-range transport of biomass burning and fossil-fuel emissions across the Southern Ocean (Seiler and Crutzen, 1980; Crutzen and Andreae, 1990; Andreae et al., 2005). Ubiquitous in the troposphere, rBC aerosols are the primary absorber of visible light impacting the Earth's radiation budget and climate (Bond and Bergstrom, 2006). Recent estimates of the globally averaged radiative forcing for rBC are as high as 1.2 Wm^2 (direct + indirect effects), the second highest radiative forcing after carbon dioxide (Ramanathan and Carmichael, 2008). However, the climate forcing from rBC in the atmosphere differs from that of greenhouse gases, which are well mixed and warm the Earth's surface. In contrast, rBC

aerosols display large spatial and temporal gradients and heat the atmosphere while cooling the surface (Ramanathan and Carmichael, 2008). The highest atmospheric concentrations of rBC are found in the tropical belt resulting from the combustion of biomass and biofuels. In the Southern Hemisphere (SH), atmospheric concentrations are highly seasonal with emissions primarily from dry-season biomass burning in Australia, southern Africa and South America (Mouillot and Field, 2005). In contrast to fossil-fuel emissions, which are highest in the northern hemisphere, biomass burning emissions are sensitive to changes in climate as well as to human activity such as tropical deforestation, land clearing, and fire suppression (Mouillot and Field, 2005). While the effects of rBC in the modern atmosphere are numerous, little is known regarding its past variability and sensitivity to climate change and human activity.

Ice core records preserve a history of rBC variability in the atmosphere with sufficient temporal-resolution to resolve seasonal changes in emission strength and atmospheric transport. Combined with general circulation modeling and rBC emission inventories, these records can provide constraints on the paleo-rBC atmospheric distribution, past biomass burning emissions and climate feedbacks (Lamarque et al., 2010; McConnell, 2010). Recent, high-temporal resolution ice core records of rBC from Greenland show that northern hemispheric rBC concentrations peaked during the early 20th Century from fossil fuel combustion (McConnell et al., 2007; McConnell, 2010) perturbing the Earth's radiation budget. While a number of paleo-biomass burning records have shown centennial scale variability in SH biomass burning (Marlon et al., 2008; Wang et al., 2010; Falk et al., 2010; Whitlock and Tinner, 2010), high temporal resolution rBC records have not been reported.

2 Ice core locations and methods

2.1 Ice core sites

The ice cores used in the study included WDC06A from West Antarctica and DSSW19K from Law Dome in East Antarctica, Table 1. The WDC06A ice core was drilled from 2007 to 2011 to a depth of ∼3330 m near the West Antarctic ice sheet divide (WAIS Divide, located ∼550 km inland). The record shown here covers the top 50.3 m of the ice core, which was drilled using an electromechanical drill in a dry bore. The DSSW19K ice core site was electromechanically drilled (dry bore) 19 km to the west of the Law Dome DSS drill site (4.7 km SSW of summit, ∼100 km inland) to a depth of 120 m in 2004. The record shown here spans the top 37 m of the ice core. Average ice accumulation rates at the sites were similar: ∼20 ± 3.4 cm a^{-1} for WDC06A, (Banta et al., 2008) and ∼15 ± 3.1 cm a^{-1} for DSSW19K. However, physical processes at DSSW19K including the formation of sastrugi (dips and ridges formed by wind erosion) limit the temporal resolution at the site to ∼1 yr while the WDC06A record was found to preserve sub-annual variability (Banta et al., 2008).

2.2 rBC ice core analysis

Longitudinal sections of the WDC06A and DSSW19K ice core were analyzed for rBC using an ice-core melter system coupled to an ultrasonic nebulization/desolation system (CETAC UT5000) (Bisiaux et al., 2011) and single particle intracavity laser induced incandescence photometer (SP 2, droplet Measurements Technologies, Boulder, Colorado). Using this method, rBC was determined in the ice core at a depth resolution of ∼1 cm corresponding to ∼25 to 35 data points per year at WAIS and ∼10 to 15 at Law Dome, although data points are not evenly distributed throughout the year because snowfall is not evenly distributed throughout the year.

2.3 Dating

Depth-age relationships for the records were developed using glaciochemistry and annual cycle counting for a suite of trace elements including sodium (Na), chloride (Cl), bromine (Br) and sulfur (S) (described in SI). Known volcanic eruptions (Tambora, Krakatoa, Agung) were also used as absolute time markers to confirm the annual layer counting. Although, extremely well preserved in the WAIS WDC06A record, annual cycles were generally less discernable in the Law Dome DSSW19K record because the net snow accumulation rate approximately equal to the height of the local surface roughness (Fig. 1 and SI-1). Cross comparisons of high resolution, continuous sulfur and sea salt measurements in the Law Dome DSS0506 and DSSW19K ice cores were used to confirm the annual layer counting. The DSS0506 core, drilled near the Law Dome DSS site in 2005 in a much higher snow accumulation rate zone and analyzed in a similar fashion but not for rBC, contains distinct annual cycles in most of the elements and chemical species we measured so dating in that core is unambiguous. While the dating uncertainty for the DSSW19K record is relatively large in comparison to WDC06A, it is sufficiently accurate to allow the calculation of net snow accumulation and rBC fluxes for both records, especially when averaged over multi-annual to decadal time scales.

3 Results and discussion

3.1 Concentrations and fluxes

Concentrations of rBC in both records were log-normally distributed (Fig. SI-2) with geometric means (geomean) of $0.8 \, \mu g \, kg^{-1}$ ($n = 4860$) and $0.9 \, \mu g \, kg^{-1}$ ($n = 2883$) for WDC06A and DSSW19K, respectively. In the WDC06A core, sub-annual rBC concentrations were highly seasonal (Fig. 1), with consistent low austral summer/fall concentrations averaging $0.04 \, \mu g \, kg^{-1}$ and high winter/spring concentrations averaging $0.15 \, \mu g \, kg^{-1}$. The DSSW19K rBC concentrations were less variable with annual

minima and maxima of 0.08 and 0.12 µg kg^{-1}, respectively. In contrast, DSSW19K rBC concentrations were more variable than WDC06A but had a comparable annual geometric mean of ∼0.08 µg kg^{-1} (Table 1). Concentrations determined in the records were comparable to the snow rBC concentrations reported by Warren and
5 Clarke (1990), Grenfell et al. (1994) and derived from a GCM model (Flanner et al., 2007), but lower than concentrations measured in older Antarctic ice by Chýlek et al. (1992), Table 1. Differences in the reported concentration range likely reflect the different time periods encompassed by the measurement and spatial variability, as well as the analytical methods used (Bisiaux et al., 2011; Kaspari et al., 2011). Annual rBC
10 fluxes, estimated from rBC concentrations and annual accumulation rate estimates were 16 ± 2.7 µg m^{-2} a^{-1} at WDC06A and 13.5 ± 2.7 µg m^{-2} a^{-1} at DSSW19K for the same time period. Integrated over the whole Antarctic continent, this corresponds to a total rBC deposition of ∼150 t a^{-1} (∼0.01 % of total rBC emission in SH estimated by Lamarque et al., 2010).

15 Time series of rBC concentrations from 1850 to 2000 are shown in Fig. 2. Both sites displayed significant annual to decadal scale variability prior to 1950. After 1950 rBC concentrations decreased until ∼1980 and then rose to pre-1950 concentrations. The decline in rBC at WDC06A during this period was not related to changes in the snow accumulation rate, which was extremely stable during this time (Banta et al., 2008).
20 At DSSWK 19, annual snow accumulation rates are less certain than WDC06A and were not used to estimate fluxes at for individual years. However, changes in the Law Dome accumulation rate have been found at the DSS ice core located 19 km from the DSS19WK site (van Ommen and Morgan, 2010). This is known to be a regionally coherent change with other records on Law Dome and in Eastern Wilkes Land showing
25 similar patterns (Morgan et al., 1991). The DSS record shows an unusual increase in snow accumulation after 1975 is found associated with changes in zonal atmospheric circulation, but no significant correlation ($R^2 = 0.07$, $p = 0.41$ for annual records and $R^2 = -0.14$, $p = 0.08$ for 5 yr smoothed records) was found between the DSS snow accumulation record and DSSWK 19 rBC and the two records appear to be unrelated.

To investigate the effect of local to regional changes in atmospheric circulation on the rBC records, the time series were compared with co-registered records of sodium (Na, a sea-salt proxy), which is modulated by both regional atmospheric transport and seasonal variability in salt emissions from the Southern Ocean by cyclonic activity and to a lesser extent from sea ice (Legrand and Mayewski, 1997; Curran et al., 1998; Goodwin et al., 2004). The records of rBC and Na at both sites were found to be autocorrelated due to a strong annual cycle, in both species. However, Na was found to lead the rBC record, by ~3 months at WDC06A and ~2 months at DSSW19K (Fig. SI-3 for the 1970–2001 period) and no correlations were found between Na records and rBC at the two sites except for the annual cycle (Fig. SI-4b). This suggests that rBC variability is not sensitive to atmospheric transport associated with cyclonic systems in the Southern Ocean, the principal source of Na in the ice core (Sneed et al., 2011). Variability of large-scale atmospheric transport (hemispheric) and source emissions at low latitudes are thus assumed to be the primary factors affecting rBC variability in the records.

Influence of ENSO

Spectral analysis of the rBC records over the 1850 to 2001 period revealed significant periodicities in the ~2 to 6 yr El Niño Southern Oscillation/Quasi-biennial oscillation band (ENSO/QBO, Fig. 3a–b) suggesting that ENSO/QBO related climate variability modulates rBC in the records (Li et al., 2011). At WDC06A, significant periodicities in the ENSO/QBO band were found at 1.7 yr (AR1 CI = 99 %) and 5 yr (AR1 CI = 90 %) while at DSSW19K significant periodicities were found at 2.3 yr (AR1 CI = 95 %) and 6 yr (AR1 CI = 95 %). These periodicities were coherent between the two sites over the 1970–2001 period (average coherence coefficient >0.38, Fig. SI-5a) suggesting a common modulation. No ENSO/QBO periodicities were found in the WDC06A Na record (Fig. SI-4a, b) further suggesting that processes driving Na at WDC06A are distinct from the modulation of rBC. On the other hand, ENSO/QBO band periodicities were found in the DSSWK 19 Na record, more influenced by the larger Na signal due

Title Page

Abstract | Introduction

Conclusions | References

Tables | Figures

|◄ | ►|

◄ | ►

Back | Close

Full Screen / Esc

Printer-friendly Version

Interactive Discussion

to the more "maritime" characteristics of DSSW19K location (Morgan et al., 1997). However, the rBC signal was found to be systematically delayed from Na by 0.3 to 2.2 yr (Fig. SI-3d).

3.2 Decadal variability: unprecedented period of low variance

On the decadal scale, the rBC records show similar features and variability, which appear to have no analogue in the ice core Na records or climatic indexes such as ENSO and the Southern Annular Mode (SAM). Notably, in the late 1950's rBC concentrations decreased abruptly (Figs. 2, 4) in parallel to the start of a low-variance period common to the two records, which persisted until ~1985 (Fig. SI-6). This period of decreased concentration and variance is consistent with rBC emissions inventories (Fig. 4) from Australia and South America grass fires (Lamarque et al., 2010) and Australia biofuel emissions (Ito and Penner, 2005). This time period also coincides with the start of Australian rational fire prevention policies (prescribed fires instead of total fire suppression), which began in the 1950's (Mouillot and Field, 2005). Similar temporal variability does not occur in the emission inventory for SH forest fires (Mouillot and Field, 2005). However, we note that recent estimates of SH rBC emissions (GFED 3, van der Werf et al., 2010) attribute ~41 % of SH rBC to grass fires (61 % if woodlands are included) with ~ 9 % from forest fires and 26 % from deforestation (primarily in South America). Thus, changes in the SH grassland (and woodland) fire regime from human activity and climate (hydroclimate) could have a significant impact on the SH rBC distribution. Emissions from SH deforestation, forest fires and fossil fuel combustion increased markedly after 1950 (Ito and Penner, 2005; Lamarque et al., 2010), Fig. 4, and may be reflected in increasing rBC concentrations observed in the last decades of the WDC06A and DSSW19K ice cores records. However, the time lag between the ice core record and rising emissions in the inventories suggest that these records may be insensitive to BC emissions transported across the Atlantic sector of the Southern Ocean.

Title Page

Abstract | Introduction

Conclusions | References

Tables | Figures

◄ | ►

◄ | ►

Back | Close

Full Screen / Esc

4 Conclusions

The high-resolution rBC ice core records in this study capture the variability of rBC deposition in two disparate regions of the Antarctic continent. These records appear to be influenced by variability similar to tropical Pacific climatic variability (ENSO) most likely due to the lagged response of grassland fuel loading to hydroclimate variability. Common variability in the records from the 1950's to 1980's was also coincident with decadal variability in grassland and biofuel rBC emission inventories (Ito and Penner, 2005; Lamarque et al., 2010). Thus, the records may be influenced by both climate variability and human activity. Further research combining general circulation model based rBC simulations with improved geospatial estimates of rBC emissions are required to deconvolve these factors. New ice core records are also required to investigate the spatial variability of rBC transport and deposition to Antarctica. In particular, development of ice core rBC records from Antarctic regions exposed to Atlantic air masses are needed to reconcile the temporal variability found in this study with increased emissions from South American deforestation and fossil-fuel combustion.

**Supplementary material related to this article is available online at:
http://www.atmos-chem-phys-discuss.net/11/27815/2011/
acpd-11-27815-2011-supplement.pdf**.

References

Andreae, M. O., Jones, C. D., and Cox, P. M.: Strong present-day aerosol cooling implies a hot future, Nature, 435, 1187–1190, 2005.

Bamber, J. L., Gomez-Dans, J. L., and Griggs, J. A.: Antarctic 1 km Digital Elevation Model (DEM) from Combined ERS-1 Radar and ICESat Laser Satellite Altimetry, Boulder, Colorado USA: National Snow and Ice Data Center, Digital Media, 2009.

Banta, J. R., McConnell, J. R., Frey, M. M., Bales, R. C., and Taylor, K.: Spatial and temporal variability in snow accumulation at the West Antarctic Ice Sheet Divide over recent centuries, J. Geophys. Res., 113, D23102, doi:10.1029/2008jd010235, 2008.

Bisiaux, M. M., Edwards, R., Heyvaert, A. C., Thomas, J. M., Fitzgerald, B., Susfalk, R. B., Schladow, S. G., and Thaw, M.: Stormwater and fire as sources of black carbon nanoparticles to Lake Tahoe, Environ. Sci. Technol., 45, 2065–2071, doi:10.1021/es103819v, 2011.

Bond, T. C. and Bergstrom, R. W.: Light Absorption by Carbonaceous Particles: An Investigative Review, Aerosol Sci. Technol., 40, 27–67, 2006.

Chýlek, P., Srivastava, V., Cahenzli, L., Pinnick, R. G., Dod, R. L., Novakov, T., Cook, T. L., and Hinds, B. D.: Aerosol and Graphitic Carbon Content of Snow, J. Geophys. Res., 92, 9801–9809, doi:10.1029/JD092iD08p09801, 1987.

Chýlek, P., Johnson, B., and Wu, H.: Black carbon concentration in Byrd station ice core – From 13,000 to 700 yr before present, Ann. Geophys., 10, 625–629, 1992, http://www.ann-geophys.net/10/625/1992/.

Crutzen, P. J. and Andreae, M. O.: Biomass burning in the tropics: Impact on atmospheric chemistry and biogeochemical cycles, Science, 250, 1669–1678, doi:10.1126/science.250.4988.1669, 1990.

Curran, M. A. J., van Ommen, T. D., and Morgan, V.: Seasonal characteristics of the major ions in the high accumulation DSS ice core, Law Dome, Antarctica, Ann. Glaciol., 22, 783–794, doi:10.1007/s00382-004-0403-3, 1998.

Falk, D. A., Heyerdahl, E. K., Brown, P. M., Swetnam, T. W., Sutherland, E. K., Gedalof, Z., Yocom, L., and Brown, T. J.: Fire and climate variation in western North America from fire-scar and tree-ring networks, PAGES News, 18, ISSM 1811–1602, 2010.

Flanner, M. G., Zender, C. S., Randerson, J. T., and Rasch, P. J.: Present-day climate forcing and response from black carbon in snow, J. Geophys. Res.-Atmos., 112, D11202, doi:10.1029/2006jd008003, 2007.

Goodwin, I. D., van Ommen, T. D., Curran, M. A. J., and Mayewski, P. A.: Mid latitude winter climate variability in the South Indian and southwest Pacific regions since 1300 AD, Clim. Dynam., 22, 783–794, doi:10.1007/s00382-004-0403-3, 2004.

Grenfell, T. C., Warren, S. G., and Mullen, P. C.: Reflection of solar-radiation by the Antarctic snow surface at ultraviolet, visible, and near-infrared wavelenghts, J. Geophys. Res.-Atmos., 99, 18669–18684, 1994.

Ito, A. and Penner, J. E.: Historical emissions of carbonaceous aerosols from biomass and fossil fuel burning for the period 1870–2000, Global Biogeochem. Cy., 19, GB2028, doi:10.1029/2004gb002374, 2005.

Kaspari, S. D., Schwikowski, M., Gysel, M., Flanner, M. G., Kang, S., Hou, S., and Mayewski, P. A.: Recent increase in black carbon concentrations from a Mt. Everest ice core spanning 1860–2000 AD, Geophys. Res. Lett., 38, L04703 doi:10.1029/2010gl046096, 2011.

Lamarque, J.-F., Bond, T. C., Eyring, V., Granier, C., Heil, A., Klimont, Z., Lee, D., Liousse, C., Mieville, A., Owen, B., Schultz, M. G., Shindell, D., Smith, S. J., Stehfest, E., Van Aardenne, J., Cooper, O. R., Kainuma, M., Mahowald, N., McConnell, J. R., Naik, V., Riahi, K., and van Vuuren, D. P.: Historical (1850–2000) gridded anthropogenic and biomass burning emissions of reactive gases and aerosols: methodology and application, Atmos. Chem. Phys., 10, 7017–7039, doi:10.5194/acp-10-7017-2010, 2010.

Legrand, M. and Mayewski, P.: Glaciochemistry of polar ice cores: A review, Rev. Geophys., 35, 219–243, doi:10.1029/96rg03527, 1997.

Li, J., Xie, S.-P., Cook, E. R., Huang, G., D'Arrigo, R., Liu, F., Ma, J., and Zheng, X.-T.: Inter-decadal modulation of El Nino amplitude during the past millennium, Nature Climate Change, 1, 114–118, 2011.

Marlon, J. R., Bartlein, P. J., Carcaillet, C., Gavin, D. G., Harrison, S. P., Higuera, P. E., Joos, F., Power, M. J., and Prentice, I. C.: Climate and human influences on global biomass burning over the past two millennia, Nat. Geosci., 1, 697–702, doi:10.1038/ngeo313, 2008.

McConnell, J. R.: New Directions: Historical black carbon and other ice core aerosol records in

the Arctic for GCM evaluation, Atmos. Environ., 44, 2665–2666, 2010.

McConnell, J. R., Edwards, R., Kok, G. L., Flanner, M. G., Zender, C. S., Saltzman, E. S., Banta, J. R., Pasteris, D. R., Carter, M. M., and Kahl, J. D. W.: 20th-century industrial black carbon emissions altered arctic climate forcing, Science, 317, 1381–1384, doi:10.1126/science.1144856, 2007.

Morgan, V. I., Goodwin, I. D., Etheridget, D. M., and Wookey, C. W.: Evidence from Antarctic ice cores for recent increases in snow accumulation, Nature, 354, 58–60, 1991.

Morgan, V. I., Wookey, C. W., Li, J., van Ommen, T. D., Skinner, W., and Fitzpatrick, M. F.: Site information and initial results from deep ice drilling on Law dome, Antarctica, J. Glaciol., 43, 3–10, 1997.

Ramanathan, V. and Carmichael, G.: Global and regional climate changes due to black carbon, Nat. Geosci., 1, 221–227, doi:10.1038/ngeo156, 2008.

Seiler, W. and Crutzen, P. J.: Estimates of gross and net fluxes of carbon between the biosphere and the atmosphere from biomass burning, Clim. Change, 2, 207–247, 1980.

Sneed, S. B., Mayewski, P. A., and Dixon, D. A.: An emerging technique: multi-ice-core multi-parameter correlations with Antarctic sea-ice extent, Ann. Glaciol., 52, 347–354, 2011.

van der Werf, G. R., Randerson, J. T., Giglio, L., Collatz, G. J., Mu, M., Kasibhatla, P. S., Morton, D. C., DeFries, R. S., Jin, Y., and van Leeuwen, T. T.: Global fire emissions and the contribution of deforestation, savanna, forest, agricultural, and peat fires (1997-2009), Atmos. Chem. Phys., 10, 11707–11735, doi:10.5194/acp-10-11707-2010, 2010

van Ommen, T. D. and Morgan, V.: Snowfall increase in coastal East Antarctica linked with southwest Western Australian drought, Nat. Geosci., 3, 267–272, 2010.

Wang, Z., Chappellaz, J., Park, K., and Mak, J. E.: Large Variations in Southern Hemisphere Biomass Burning During the Last 650 Years, Science, 330, 1663–1666, doi:10.1126/science.1197257, 2010.

Warren, S. G. and Clarke, A. D.: Soot in the atmosphere and snow surface of Antarctica, J. Geophys. Res.-Atmos., 95, 1811–1816, 1990.

Whitlock, C. and Tinner, W.: Editorial: Fire in the Earth System, Pages News, 18, 55–56, 2010.

Large scale changes in 20th century black carbon deposition to Antarctica

M. M. Bisiaux et al.

Title Page

Abstract	Introduction
Conclusions	References
Tables	Figures

◄◄ ►►

◄ ►

Back Close

Full Screen / Esc

Printer-friendly Version

Interactive Discussion

Table 1. Ranges and averages of annual rBC concentrations for this study and previous work in Greenland and Antarctica (snow and ice). Approximate location of WDC06A and DSSW19K sites are shown on the map on left hand corner.

	Location		Lat/long	Elevation (ASL)	Age of sample (in Cal. yr or as specified)	Annual concentrations (μg/kg)		Method
						Range[a]	Average[a]	
This study	Antarctica	WAIS (WDC06A)	79.46° S, 112.08° W	1766 m	1970–2000	0.03 to 0.30	0.08	SP2-FIA
"	"	"	"	"	1850–2000	0.03 to 0.30	0.08	
"	Antarctica	Law Dome (DSSW19K)	66.78° S, 112.37° E	1230 m[b]	1970–2000	0.02 to 0.32	0.08	
"	"	"	"	"	1850-d-2000	0.01 to 0.55	0.09	
McConnell et al. (2007)	Greenland	D4	71.4° N, 44.0° W	2710 m	1952–2002	< 1 to 10	2.3	Transmittance on quartz fiber filter
"	"	"	"	"	1851–1951	~1 to 20	4	
Chylek et al. (1995)	Greenland	Summit/GISP2	72.36° N, 38.30° W	3200 m	320–330	0.5 to 6.5	2.1	
"	"	"	"	"	recent snow	–	2	
Chylek et al. (1987)	Greenland	Camp Century	78.85° N, 55.232° W	2000 m	4 kyrBP	–	2.5	
"	"	"	"	"	6 kyrBP	–	1.1	
"	Antarctica	Siple Dome	81.66° S, 148.83° W	1050 m	recent snow	–	2.5	
Chylek et al. (1992)	Antarctica	Byrd station	80.02° S, 119.53° W	1550 m	0.7 to 10 kyrBP	0.1 to 0.95	0.5	
"	Antarctica	"	"	"	10 to 14 kyrBP	0.1 to 0.4	0.2	
Warren and Clarke (1990)	Antarctica	South Pole station	90° S, 0° W	2830 m	recent snow	0.1 to 0.3	0.2	
Grenfell et al. (1994)	Antarctica	"	"	"	recent snow	0.1 to 0.3	0.3	
Grenfell et al. (1994)	Antarctica	Vostok	78.46° S, 106.83° W	3488 m	recent snow	1 to 7	(Contamination)	

[a] For this work only, annual concentrations are calculated from the log values of monthly data and the average is the geometric mean of those annual concentrations. For Law Dome, out-layer year 1910 has been excluded of range estimation.
[b] Altitude measured by Digital Elevation Model from (Bamber et al., 2009).
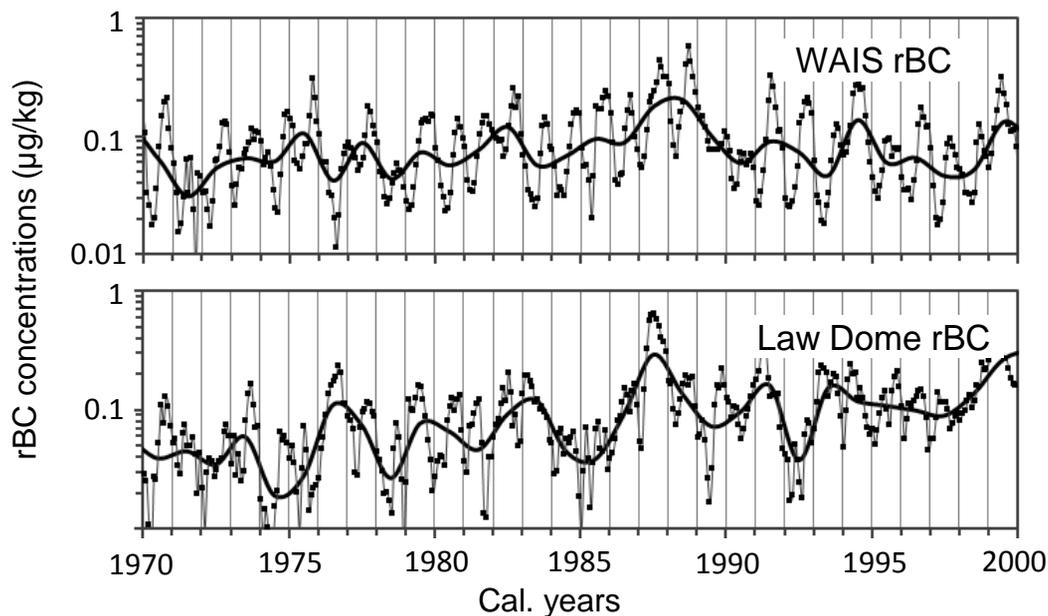
Fig. 1. 1970–2000 monthly (dots) and annual smoothing (line) for rBC at WAIS and Law Dome.
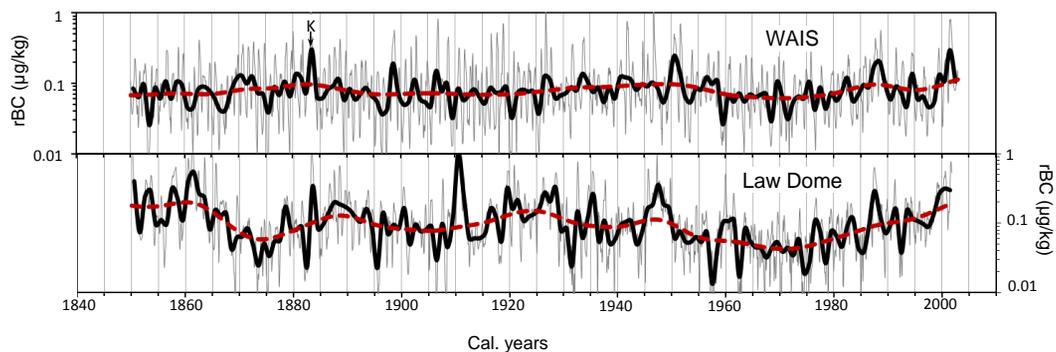
Fig. 2. Smoothed rBC concentrations (thick) and decimal (thin) for WAIS (top) and Law Dome (bottom), re-sampled with a piece-wise linear interpolation integration. Red dash line is 21 yr smoothing with R implementation of Nadaraya-Watson kernel regression estimate. K marks the Krakatoa volcanic eruption used for dating.
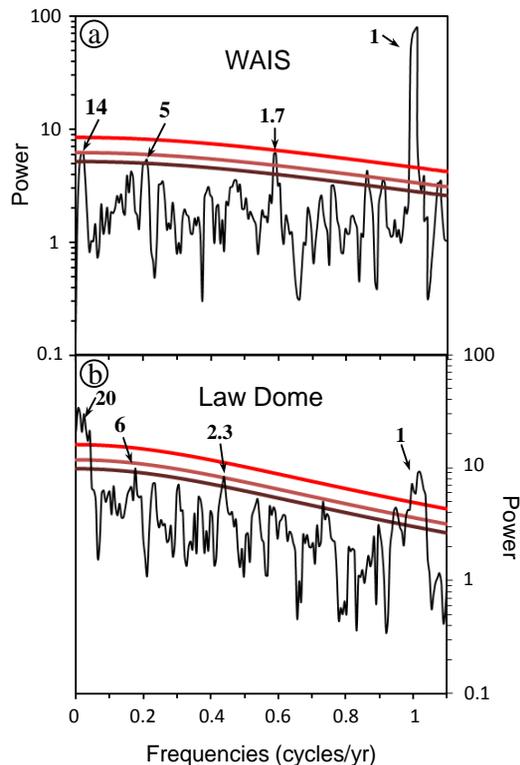
Fig. 3. Spectrums obtained by Multi taper Method (MTM), for WAIS **(a)** and Law Dome **(b)** monthly rBC records for 1850–2001 period and confidence levels in red lines (90, 95, 99 %). Significant periodicities (notably in ENSO and QBO band) an corresponding values in years are indicated as numbers on the graph.
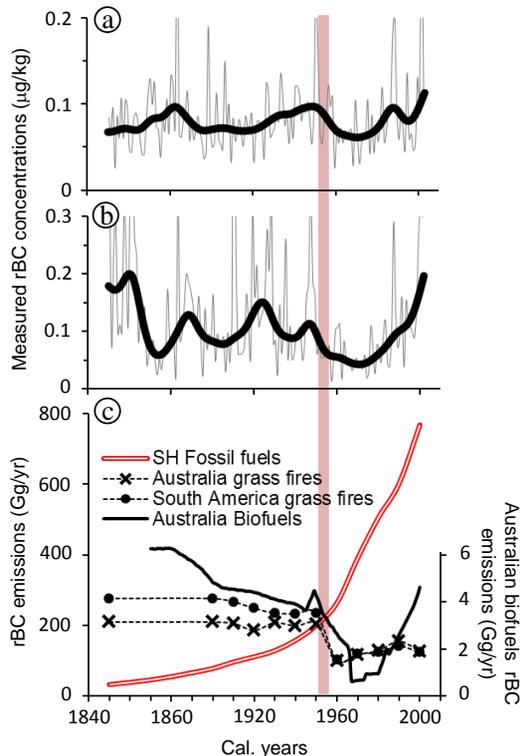
Fig. 4. **(a, b)** rBC records for WAIS and Law Dome. In gray, concentrations re-sampled to annual resolution with a piece-wise linear interpolation integration. Dark thick lines are 21 yr smoothing with *R* implementation of Nadaraya-Watson kernel regression estimate. **(c)** comparison with reconstructed rBC emissions from SH fossil fuel anthropogenic use, Australian grass fires, South American grass fires (Lamarque et al. 2010) – left scale – and from Australian biofuels (Ito and Penner, 2005) – right scale. The vertical bar highlights the beginning of fire prevention in Australia.

Large scale changes in 20th century black carbon deposition to Antarctica

M. M. Bisiaux et al.

Title Page

Abstract	Introduction
Conclusions	References
Tables	Figures

◀ | ▶

◀ | ▶

Back | Close

Full Screen / Esc

Printer-friendly Version

Interactive Discussion